Application of Roe's Scheme to the Shallow Water Equations on the Sphere

Amanda Crossley

September 1994

Submitted to the

Department of Mathematics,

University of Reading,

in partial fulfillment of the requirements for the

Degree of Master of Science.

Abstract

In this dissertation we use an upwind finite difference method known as Roe's scheme to solve the flux form of the shallow water equations over a sphere explicitly. The shallow water equations are transformed into a set of conservation laws, together with source terms as a result of the earth's rotation and the presence of mountains on the earth's surface. We incorporate the technique of operator splitting on a regular longitude latitude grid to allow the method to be applied to the two-dimensional shallow water equations. As a result of the first order scheme being highly diffusive we observe the need to use a second order version of Roe's method which incorporates a flux limiter. The method is applied to a standard test case in numerical weather prediction.

Contents

Chapter 1

Introduction

The weather is a very important factor in many peoples lives, so it is of great interest to know what the weather will be like in advance. Thus there is a need to be able to predict the weather, as it has a great influence on society.

In order to make predictions, mathematical models must be formed. In forming any model, it must be decided exactly what it is that is being modelled, and what factors are involved. Once the factors have been decided, a way must be found to quantify them. Only then may the laws and relationships be postulated which characterise the model. Often the result is a set of complicated differential equations for which there is no analytical solution. If this is the case then numerical techniques must be applied to find a solution to the problem.

Within the atmosphere many complex processes take place. Even if it is desired to model a particular process, quite often it is not possible to isolate that process from all of the others, and some combined effect must been considered.

Numerical weather prediction involves solving numerically a large set of differential equations. Even though certain assumptions and simplifications will have

been made to derive the equations, the problem is still a complex one, and finding the solution poses many difficulties. Meteorologists are always looking to improve the numerical methods used to study the weather. Applying different numerical schemes to the problem may yield different results. A decision must be made as to what properties are desirable in a scheme and at what computational expense these can be attained. This gives an indication of the performance of a particular scheme in terms of its properties. Another way to draw a comparison between different methods is to apply the methods to much simpler problems which somehow reflect the behaviour of a larger system, perhaps to a problem where the analytic solution is known. Such a problem is referred to as a test case. Should a particular method fail to work well with a test case, then it almost certainly will not work with a more difficult problem. However should the results look promising then there is a chance that the method will work when applied to a more complex system.

In atmospheric modelling one such test case is the shallow water equations. The shallow water equations describe the depth and velocity profiles of an inviscid fluid. They are derived from the Navier-Stokes equations by assuming that the vertical component of the acceleration of the fluid flow is zero, and by intergrating the resulting equations over the depth of the fluid [4]. This leads to a two-dimensional problem.

A particular problem encountered in numerical weather prediction on longitude/latitude grids is occurrence of singularities at the poles. This is a consequence of using a numerical grid which has nodes at the poles. At such points the grid lines meet and there is a difficulty in defining specific quantities as the infor-

mation conveyed from the different latitudinal lines may conflict. One solution to this problem is of course not to have grid points at the poles.

The poles can again present a problem when regular grids are used, as the grid points bunch together in their vicinity. When explicit finite difference methods are used, this imposes the need for a smaller time step at the poles than required elsewhere on the grid, in order to satisfy the Courant-Friedrichs-Lewy (CFL) stability condition.

The purpose of this project is to implement an upwind TVD scheme, namely Roe's scheme, for the shallow water equations on a rotating sphere, which is a standard test case in numerical weather prediction. In the following section Roe's scheme will be discussed and its advantages and disadvantages over other methods considered. Chapter 3 deals with the shallow water equations and the manipulation involved to enable the implementation of the method. A test case is then presented, the results from which are shown. Finally a discussion is given on the conclusions drawn from the project.

Chapter 2

Roe's method

2.1 Roe's scheme

Roe [8] proposed a method to obtain an approximate solution to a set of conservation laws of the form

$$\mathbf{w}_t + \mathbf{F}_x = 0 \tag{2.1}$$

based on regarding the data as piecewise constant and solving a set of Riemann problems. A Riemann problem is one where the initial data is constant either side of a discontinuity. If the discontinuity lies at the point $x = x'$ then the initial values are

$$\mathbf{w}(0, x) = \begin{cases} \mathbf{w}_L & \text{if } x < x' \\ \mathbf{w}_R & \text{if } x > x' \end{cases} \tag{2.2}$$

where $\mathbf{w}_L$ and $\mathbf{w}_R$ denote the left and right states and x' is the interface between them.

The solution to equation (2.1), $\mathbf{w}_j^n$, is regarded as an approximation to the average state between two interfaces, where the interfaces are placed at the mid

points of the cells, i.e.

$$\mathbf{w}_j^n = \frac{1}{\Delta x} \int_{(i-\frac{1}{2})dx}^{(i+\frac{1}{2})\Delta x} \mathbf{w}(x, n\Delta t)dx \tag{2.3}$$

where Δx is the grid spacing on a regular grid, and Δt is the time step.

If the problem (2.1) is approximated by

$$\mathbf{w}_t + \tilde{A}\mathbf{w}_x = 0 \tag{2.4}$$

where $\tilde{A}$ is a constant matrix, then an approximate solution to the exact problem (2.1) can be taken to be the exact solution to the approximate problem (2.4).

The matrix $\tilde{A}$ which depends on $\mathbf{w}_L$ and $\mathbf{w}_R$, can be picked in many ways but in Roe's scheme is chosen so that it satisfies the following properties.

(i) $\tilde{A}$ constitutes a linear mapping from the vector space $\mathbf{w}$ to the vector space $\mathbf{F}$.

(ii) As $\mathbf{w}_L \to \mathbf{w}_R \to \mathbf{w}$, $\tilde{A}(\mathbf{w}_L, \mathbf{w}_R) \to A(\mathbf{w})$, where $A = \dfrac{\partial \mathbf{F}}{\partial \mathbf{w}}$.

(iii) For any $\mathbf{w}_L$, $\mathbf{w}_R$, $\tilde{A}(\mathbf{w}_L, \mathbf{w}_R) \times (\mathbf{w}_L - \mathbf{w}_R) = \mathbf{F}_L - \mathbf{F}_R$.

(iv) The eigenvectors of $\tilde{A}$ are linearly independent.

The above set of conditions, termed 'Property U' by Roe [8] ensures that the Riemann solver has the desirable properties that the solution is consistent and conservative and therefore gives the correct shock speeds across a shock.

For any two states, $\mathbf{w}_L$ and $\mathbf{w}_R$, the flux difference can be expressed as [11]

$$\mathbf{F}_R - \mathbf{F}_L = \sum_k \tilde{\alpha}_k \tilde{\lambda}_k \tilde{\mathbf{e}}_k \tag{2.5}$$

where $\tilde{\mathbf{e}}_k$ are the right eigenvectors of $\tilde{A}$, $\tilde{\lambda}_k$ are the eigenvalues or wave speeds and $\tilde{\alpha_k}$ are coefficients known as the wave strengths. This results in the flux at

the interface being

$$\mathbf{F}_{i+\frac{1}{2}}(\mathbf{w}_L, \mathbf{w}_R) = \frac{1}{2}(\mathbf{F}_L + \mathbf{F}_R) - \frac{1}{2}\sum_k \tilde{\alpha}_k \left|\tilde{\lambda}_k\right| \tilde{\mathbf{e}}_k. \tag{2.6}$$

For linear problems, this is equivalent to the early Courant-Isaacson-Rees (CIR) method [1].

To apply the method to a non-linear problem, the local linearisation described above can be introduced by choosing $\tilde{A}$ having property U which implies that its eigenvalues and eigenvectors not only satisfy equation (2.5) but also

$$\mathbf{w}_R - \mathbf{w}_L = \sum_k \tilde{\alpha}_k \tilde{\mathbf{e}}_k. \tag{2.7}$$

Each $\tilde{\alpha}$ satisfies a scalar scheme and the method of updating is to

$$\text{add } -\frac{\Delta t}{\Delta x}\tilde{\lambda}_k \tilde{\alpha}_k \tilde{\mathbf{e}}_k \text{ to } \mathbf{w}_R \text{ if } \tilde{\lambda}_k > 0 \tag{2.8}$$

and

$$\text{add } -\frac{\Delta t}{\Delta x}\tilde{\lambda}_k \tilde{\alpha}_k \tilde{\mathbf{e}}_k \text{ to } \mathbf{w}_L \text{ if } \tilde{\lambda}_k < 0 \tag{2.9}$$

where $\tilde{\lambda}_k$, $\tilde{\alpha}_k$ and $\tilde{\mathbf{e}}_k$ are determined in the calculation using the values of $\mathbf{w}$ and $\mathbf{F}$ from the current time step, and so the method is explicit.

2.2 Why use Roe's scheme?

In this instance the main advantages of using Roe's scheme are that it allows the use of upwinding which preserves monotonicity of the solution, and of course it is also conservative.

When applied to scalar problems, Roe's method is the same as the first order upwind method, yielding only first order accurate results that are free of oscillations. Often in a general problem where greater accuracy is required, central

differences would be used to approximate the spatial derivatives. However in the case of hyperbolic conservation laws, using central differences results in a unconditionally unstable scheme, when applied explicitly. Although implicit central difference schemes have no stability limits, they can be much more computationally expensive to use than explicit methods and can also suffer from oscillations.

Another possibility is the Lax-Wendroff method. This scheme is explicit, second order and conditionally stable. However the method is also prone to oscillations which can give non-physical solutions, such as negative depth. Roe's scheme can be made second order by the introduction of a flux limiter [12]. Limiters add an anti diffusive term to the scheme which helps reduce the effects of diffusion, whilst maintaining an oscillation free method.

2.3 Application to 2-d problems

To enable Roe's scheme to be applied to a system in 2-d, the equations must be decomposed into a set of one dimensional problems. One technique for achieving this is known as 'operator splitting' (see [2] for application to the Euler equations). For the system of equations

$$\mathbf{w}_t + \mathbf{F}_x + \mathbf{G}_y = 0, \tag{2.10}$$

applying the use of operator splitting in its simplest form results in the following 1-d problems

$$\frac{1}{2}\mathbf{w}_t + \mathbf{F}_x = 0 \tag{2.11}$$

$$\frac{1}{2}\mathbf{w}_t + \mathbf{G}_y = 0. \tag{2.12}$$

At each time step, the solution to equations (2.11) and (2.12) are found in turn over the region and superimposed to obtain the approximate solution of (2.10).

Another more complex form of splitting which can be used to obtain the decomposition is 'Strang splitting'. This is similar to the splitting described above in that it involves rewriting the problem as a set of equations which are similar in form to equations (2.11) and (2.12). The difference between the two types lies in the order in which the equations are solved and in the size of the time step used. If we represent the problem in equation (2.10) using the simpler form of splitting as

$$L^x_{\frac{1}{2}\Delta t} L^y_{\frac{1}{2}\Delta t}$$

where $L^x_{\frac{1}{2}\Delta t}$ represents equation (2.11) and likewise $L^y_{\frac{1}{2}\Delta t}$ is equation (2.12), then the application of Strang splitting to the problem can be denoted by

$$L^x_{\frac{1}{4}\Delta t} L^y_{\frac{1}{4}\Delta t} L^y_{\frac{1}{4}\Delta t} L^x_{\frac{1}{4}\Delta t}$$

which is equivalent to

$$L^x_{\frac{1}{4}\Delta t} L^y_{\frac{1}{2}\Delta t} L^x_{\frac{1}{4}\Delta t}$$

so that we solve the problem along the x coordinate direction using a quarter time step, then the y direction using a half time step and then finally solve again along the x direction using a quarter time step.

Chapter 3

The equations

3.1 Standard form of the shallow water equations equations

In flux form (with source terms) the shallow water equations on a rotating sphere can be written as [13]

$$\frac{\partial(h^*\mathbf{v})}{\partial t} + \nabla.(\mathbf{v}h^*\mathbf{v}) = -f\hat{\mathbf{k}} \times h^*\mathbf{v} - gh^*\mathbf{v}\nabla h \tag{3.1}$$

and

$$\frac{\partial h^*}{\partial t} + \nabla.(h^*\mathbf{v}) = 0, \tag{3.2}$$

where h^* is the depth of the fluid and h is the height of the free surface above a reference sphere i.e. sea level. If h_s represents the heights of any mountains present then $h = h^* + h_s$. The horizontal vector velocity, $\mathbf{v}$, has components u and v in the longitudinal (ϕ) and latitudinal (θ) directions respectively. The radius of the earth is labelled a, and g is the gravitational constant. The Coriolis parameter, f, is given by $f = 2\Omega \sin\theta$ where Ω is the rate of rotation of the earth.

Using $\mathbf{i}$, $\mathbf{j}$ and $\mathbf{k}$ to denote the longitudinal, latitudinal and outward radial unit vectors respectively, the horizontal vector velocity is represented as $\mathbf{v} = u\mathbf{i} + v\mathbf{j}$ and the spherical horizontal gradient and divergence operators become

$$\nabla h \equiv \frac{\mathbf{i}}{a\cos\theta}\frac{\partial h}{\partial \phi} + \frac{\mathbf{j}}{a}\frac{\partial h}{\partial \theta} \tag{3.3}$$

and

$$\nabla.\mathbf{v} \equiv \frac{1}{a\cos\theta}\left[\frac{\partial u}{\partial \phi} + \frac{\partial (v\cos\theta)}{\partial \theta}\right]. \tag{3.4}$$

If equation (3.1) is written in terms of the velocity components then after some rearrangement, the resulting equations are

$$\frac{\partial (h^* u)}{\partial t} + \nabla.(h^* u\mathbf{v}) + \frac{gh^*}{a\cos\theta}\frac{\partial h}{\partial \phi} = \left(f + \frac{u}{a}\tan\theta\right) h^* v \tag{3.5}$$

and

$$\frac{\partial (h^* v)}{\partial t} + \nabla.(h^* v\mathbf{v}) + \frac{gh^*}{a}\frac{\partial h}{\partial \theta} = -\left(f + \frac{u}{a}\tan\theta\right) h^* u. \tag{3.6}$$

Expanding the divergence terms then gives

$$\frac{\partial h^*}{\partial t} + \frac{1}{a\cos\theta}\left[\frac{\partial (h^* u)}{\partial \phi} + \frac{\partial (h^* v\cos\theta)}{\partial \theta}\right] = 0 \tag{3.7}$$

$$\frac{\partial (h^* u)}{\partial t} + \frac{1}{a\cos\theta}\left[\frac{\partial (h^* u^2)}{\partial \phi} + \frac{\partial (h^* uv\cos\theta)}{\partial \theta}\right] + \frac{gh^*}{a\cos\theta}\frac{\partial h}{\partial \phi} = \left(f + \frac{u}{a}\tan\theta\right) h^* v \tag{3.8}$$

$$\frac{\partial (h^* v)}{\partial t} + \frac{1}{a\cos\theta}\left[\frac{\partial (h^* uv)}{\partial \phi} + \frac{\partial (h^* v^2\cos\theta)}{\partial \theta}\right] + \frac{gh^*}{a}\frac{\partial h}{\partial \theta} = -\left(f + \frac{u}{a}\tan\theta\right) h^* u. \tag{3.9}$$

3.2 Obtaining the conservation form

As they stand, equations (3.7) to (3.9) are not in the form required to apply Roe's method. We now proceed to derive the equations in conservation law form as far

as possible. Firstly, multiplying the equations through by $\cos\theta$, and introducing a new variable h' where $h' = h^* \cos\theta$, we obtain

$$\frac{\partial h'}{\partial t} + \frac{\partial}{\partial \theta}\left(\frac{h'u}{a\cos\theta}\right) + \frac{\partial}{\partial \theta}\left(\frac{h'v}{a}\right) = 0 \tag{3.10}$$

$$\frac{\partial}{\partial t}(h'u) + \frac{\partial}{\partial \phi}\left(\frac{h'uv}{a\cos\theta}\right) + \frac{\partial}{\partial \theta}\left(\frac{h'v^2}{a}\right) + \frac{gh'}{a\cos\theta}\frac{\partial h}{\partial \phi} = \left(f + \frac{u}{a}\tan\theta\right)h'v \tag{3.11}$$

$$\frac{\partial}{\partial t}(h'v) + \frac{\partial}{\partial \phi}\left(\frac{h'uv}{a\cos\theta}\right) + \frac{\partial}{\partial \theta}\left(\frac{h'v^2}{a}\right) + \frac{gh'}{a}\frac{\partial h}{\partial \theta} = -\left(f + \frac{u}{a}\tan\theta\right)h'u. \tag{3.12}$$

By substituting $h = h^* + h_s$ into equations (3.11) and (3.12), the partial derivatives involving h can be split up, and after some manipulation and rearrangement, equations (3.11) and (3.12) become

$$\frac{\partial}{\partial t}(h'u) + \frac{\partial}{\partial \phi}\left(\frac{h'u^2}{a\cos\theta} + \frac{h'^2 g}{2a\cos^2\theta}\right) + \frac{\partial}{\partial \theta}\left(\frac{h'uv}{a}\right) = \left(f + \frac{u\tan\theta}{a}\right)h'v - \frac{gh'}{a\cos\theta}\frac{\partial h_s}{\partial \phi} \tag{3.13}$$

$$\frac{\partial}{\partial t}(h'v) + \frac{\partial}{\partial \phi}\left(\frac{h'uv}{a\cos\theta}\right) + \frac{\partial}{\partial \theta}\left(\frac{h'v^2}{a} + \frac{h'^2 g}{2a\cos\theta}\right) = -\left(f + \frac{u\tan\theta}{a}\right)h'u - \frac{gh'}{a}\frac{\partial h_s}{\partial \theta} - \frac{h'^2 g}{2a}\frac{\tan\theta}{\cos\theta}. \tag{3.14}$$

Together with equation (3.10), these can now be written as the matrix system

$$\mathbf{w}_t + \mathbf{F}_\phi + \mathbf{G}_\theta = \mathbf{f} + \mathbf{g} + \mathbf{s} \tag{3.15}$$

where

$$\mathbf{w} = (h', h'u, h'v)^T \tag{3.16}$$

$$\mathbf{F} = \left(\frac{h'u}{a\cos\theta}, \frac{h'u^2}{a\cos\theta} + \frac{h'^2 g}{2a\cos^2\theta}, \frac{h'uv}{a\cos\theta}\right)^T \tag{3.17}$$

$$\mathbf{G} = \left(\frac{h'v}{a}, \frac{h'uv}{a}, \frac{h'v^2}{a} + \frac{h'^2 g}{2a\cos\theta}\right)^T \tag{3.18}$$

$$\mathbf{f} = \left(0, -\frac{gh'}{a\cos\theta}\frac{\partial h_s}{\partial \phi}, 0\right)^T \tag{3.19}$$

$$\mathbf{g} = \left(0, 0, -\frac{gh'}{a}\frac{\partial h_s}{\partial \theta}\right)^T \tag{3.20}$$

$$\mathbf{s} = \left(0, h'v\left(f + \frac{u\tan\theta}{a}\right), -h'u\left(f + \frac{u\tan\theta}{a}\right) - \frac{h'^2 g\tan\theta}{2a\cos\theta}\right)^T. \tag{3.21}$$

3.3 Application of Roe's method

Following along the lines of previous work by Glaister ([2],[3]) we proceed to apply Roe's method. Using the method of operator splitting, the two equations to be solved are

$$\frac{1}{2}\mathbf{w}_t + \mathbf{F}_\phi = \mathbf{f} + \frac{1}{2}\mathbf{s} \tag{3.22}$$

and

$$\frac{1}{2}\mathbf{w}_t + \mathbf{G}_\phi = \mathbf{g} + \frac{1}{2}\mathbf{s}. \tag{3.23}$$

However, in applying Roe's scheme, only the source terms found in $\mathbf{f}$ and $\mathbf{g}$ will be included in the first instance, i.e. the method will be applied to the problems

$$\frac{1}{2}\mathbf{w}_t + \mathbf{F}_\phi = \mathbf{f} \tag{3.24}$$

$$\frac{1}{2}\mathbf{w}_t + \mathbf{G}_\phi = \mathbf{g}. \tag{3.25}$$

The source terms found in $\mathbf{s}$, which result from the earths rotation, can be accounted for after equations (3.24) and (3.25) have been solved.

First let us consider equation (3.24)

3.3.1 Applying to the longitudinal (ϕ) direction

In order to find A, the Jacobian of $\mathbf{F}$, the vector $\mathbf{w}$ is redefined as

$$\mathbf{w} = (h', m, n)^T \tag{3.26}$$

where $m = h'u$ and $n = h'v$. In terms of these variables, $\mathbf{F}$ is now

$$\mathbf{F} = \left(\frac{m}{a\cos\theta}, \frac{m^2}{ah'\cos\theta} + \frac{h'^2 g}{2a\cos^2\theta}, \frac{mn}{ah'\cos\theta} \right)^T . \tag{3.27}$$

From these definitions of $\mathbf{w}$ and $\mathbf{F}$, the Jacobian of $\mathbf{F}$ is

$$A = \frac{\partial \mathbf{F}}{\partial \mathbf{w}} = \begin{pmatrix} 0 & \frac{1}{a\cos\theta} & 0 \\ -\frac{m^2}{ah'^2\cos\theta} + \frac{h'g}{a\cos^2\theta} & \frac{2m}{ah'\cos\theta} & 0 \\ -\frac{mn}{ah'^2\cos\theta} & \frac{n}{ah'\cos\theta} & \frac{m}{ah'\cos\theta} \end{pmatrix} \tag{3.28}$$

or, in terms of the original variables,

$$A = \begin{pmatrix} 0 & \frac{1}{a\cos\theta} & 0 \\ -\frac{u^2}{a\cos\theta} + \frac{h'g}{a\cos^2\theta} & \frac{2u}{a\cos\theta} & 0 \\ -\frac{uv}{a\cos\theta} & \frac{v}{a\cos\theta} & \frac{u}{a\cos\theta} \end{pmatrix} . \tag{3.29}$$

The eigenvalues of A are then found to be

$$\lambda_1 = \frac{u}{a\cos\theta} + \frac{\sqrt{h^* g}}{a\cos\theta} \ , \ \lambda_2 = \frac{u}{a\cos\theta} - \frac{\sqrt{h^* g}}{a\cos\theta} \ , \ \lambda_3 = \frac{u}{a\cos\theta}, \tag{3.30}$$

with corresponding eigenvectors

$$\mathbf{e}_1 = \begin{pmatrix} 1 \\ u + \sqrt{h^* g} \\ v \end{pmatrix} \ , \ \mathbf{e}_2 = \begin{pmatrix} 1 \\ u - \sqrt{h^* g} \\ v \end{pmatrix} \ , \ \mathbf{e}_3 = \begin{pmatrix} 0 \\ 0 \\ 1 \end{pmatrix} . \tag{3.31}$$

Having found exact expressions for the Jacobian and its eigenvalues and eigenvectors, we can proceed to find the wavestrengths for two adjacent states $\mathbf{w}_L$ and $\mathbf{w}_R$, i.e. to find α_1, α_2 and α_3 such that

$$\Delta \mathbf{w} = \sum_{k=1}^{3} \alpha_k \mathbf{e}_k \tag{3.32}$$

and also (using property U)

$$\Delta \mathbf{F} = \sum_{k=1}^{3} \lambda_k \alpha_k \mathbf{e}_k, \tag{3.33}$$

where $\Delta(.) = (.)_R - (.)_L$ denotes the difference between the right and left states. From our definition of $\mathbf{w}$ this leads to the following conditions,

$$\Delta h' = \alpha_1 + \alpha_2 \tag{3.34}$$

$$\Delta(h'u) = \alpha_1\left(u + \sqrt{h^* g}\right) + \alpha_2\left(u - \sqrt{h^* g}\right) \tag{3.35}$$

$$\Delta(h'v) = \alpha_1 v + \alpha_2 v + \alpha_3. \tag{3.36}$$

Substitution for α_1, α_2 and α_3 yields the following expressions for the wavestrengths

$$\alpha_1 = \frac{1}{2}\Delta h' + \frac{1}{2\sqrt{h^* g}}\left[\Delta(h'u) - u\Delta h'\right] \tag{3.37}$$

$$\alpha_2 = \frac{1}{2}\Delta h' - \frac{1}{2\sqrt{h^* g}}\left[\Delta(h'u) - u\Delta h'\right] \tag{3.38}$$

$$\alpha_3 = \Delta(h'v) - v\Delta h'. \tag{3.39}$$

The approximate problem

In applying the method, it is not equation (3.24) that is solved, but its approximation over the interval $[\phi_L, \phi_R]$. The vectors $\mathbf{w}_L$ and $\mathbf{w}_R$ are the approximations to $\mathbf{w}$ at the points ϕ_L and ϕ_R which lie either side of the interface positioned at $\frac{1}{2}(\phi_L + \phi_R)$. The problem to be solved is

$$\frac{\mathbf{w}_P^{n+1} - \mathbf{w}_P^n}{\Delta t} + \tilde{A}\frac{(\mathbf{w}_R - \mathbf{w}_L)}{\Delta\phi} = \tilde{\mathbf{f}}\left(\mathbf{w}^n\right) \tag{3.40}$$

where P corresponds to either the left or the right state, L or R. $\tilde{A}$ is the approximation to the Jacobian and $\tilde{\mathbf{f}}$ approximates the source terms due to the mountains. We shall choose $\tilde{\mathbf{f}}$ to be

$$\tilde{\mathbf{f}} = \left(0, -\frac{g\tilde{h}'}{a\cos\theta}\frac{\Delta h_s}{\Delta\phi}, 0\right)^T. \tag{3.41}$$

Rearranging equation (3.40) gives

$$\mathbf{w}_P^{n+1} = \mathbf{w}_P^n + \Delta t \tilde{\mathbf{f}} - \frac{\Delta t}{\Delta \phi} \tilde{A} \left(\mathbf{w}_R - \mathbf{w}_L \right). \tag{3.42}$$

To find the new value of $\mathbf{w}_P$ at the next time step, $(\mathbf{w}_R - \mathbf{w}_L)$ and $\tilde{\mathbf{f}}$ are projected onto the local eigenvectors. If

$$\mathbf{w}_R - \mathbf{w}_L = \sum_{k=1}^{3} \tilde{\alpha}_k \tilde{\mathbf{e}}_k \tag{3.43}$$

then

$$\tilde{A} \left(\mathbf{w}_R - \mathbf{w}_L \right) = \sum_{k=1}^{3} \tilde{\lambda}_k \tilde{\alpha}_k \tilde{\mathbf{e}}_k \tag{3.44}$$

where

$$\tilde{A} \Delta \mathbf{w} = \Delta \mathbf{F} \tag{3.45}$$

Moreover, expanding the source term in terms of the eigenvectors of $\tilde{A}$

$$\tilde{\mathbf{f}} \left(\mathbf{w}^n \right) = -\frac{1}{\Delta \phi} \sum_{k=1}^{3} \tilde{\beta}_k \tilde{\mathbf{e}}_k \tag{3.46}$$

enables equation (3.42) to be rewritten as

$$\mathbf{w}_P^{n+1} = \mathbf{w}_P^n + \frac{\Delta t}{\Delta \phi} \sum_{k=1}^{3} \tilde{\lambda}_k \tilde{\gamma}_k \tilde{\mathbf{e}}_k \tag{3.47}$$

where $\tilde{\gamma}_k = \tilde{\alpha}_k + \tilde{\beta}_k / \tilde{\lambda}_k$.

To perform the update, each interface (or cell) is considered in turn. For a specific cell, either $\mathbf{w}_L$ or $\mathbf{w}_R$ will be incremented, depending on the sign of the eigenvalue. The result is that we

$$\text{add } -\frac{\Delta t}{\Delta \phi} \tilde{\lambda}_k \tilde{\gamma}_k \tilde{\mathbf{e}}_k \text{ to } \mathbf{w}_R \text{ if } \tilde{\lambda}_k > 0 \tag{3.48}$$

or

$$\text{add } -\frac{\Delta t}{\Delta \phi} \tilde{\lambda}_k \tilde{\gamma}_k \tilde{\mathbf{e}}_k \text{ to } \mathbf{w}_L \text{ if } \tilde{\lambda}_k < 0 \tag{3.49}$$

where $\tilde{\lambda}_k$, $\tilde{\gamma}_k$ and $\tilde{\mathbf{e}}_k$ are to be determined.

Approximate values for the Riemann solver

We now go on to find approximate values for the variables at the interface states based on the left and right values at the grid points. The approximate values for the eigenvalues, eigenvectors and wavestrengths within a cell are found by substituting the approximate values for u, v and $\sqrt{h^* g}$ at the interface into the expressions for the exact values of λ_k, $\mathbf{e}_k$ and α_k. Thus it remains to find approximations for u, v, h' and $\sqrt{h^* g}$ at the mid points of the cells.

Let $\tilde{\psi}^2$ denote the approximation to $\sqrt{h^* g}$, then from equations (3.44) and (3.45) and, after multiplication through by $\cos\theta$, the following expressions are obtained

$$\Delta(h'u) = \left(\tilde{u} + \tilde{\psi}\right)\tilde{\alpha}_1 + \left(\tilde{u} - \tilde{\psi}\right)\tilde{\alpha}_2 \tag{3.50}$$

$$\Delta\left(h'u^2 + \frac{h'^2 g}{2\cos\theta}\right) = \left(\tilde{u} + \tilde{\psi}\right)^2\tilde{\alpha}_1 + \left(\tilde{u} - \tilde{\psi}\right)^2\tilde{\alpha}_2 \tag{3.51}$$

$$\Delta(h'uv) = \left(\tilde{u} + \tilde{\psi}\right)\tilde{v}\tilde{\alpha}_1 + \left(\tilde{u} - \tilde{\psi}\right)\tilde{v}\tilde{\alpha}_2 + \tilde{u}\tilde{\alpha}_3, \tag{3.52}$$

where a tilde above a value denotes its approximation.

By expanding the brackets in equation (3.51) and rearranging the right hand side, the equation becomes

$$\Delta\left(h'u^2 + \frac{h'^2 g}{2a\cos\theta}\right) = \left(\tilde{u}^2 + \tilde{\psi}^2\right)(\tilde{\alpha}_1 + \tilde{\alpha}_2) + 2\tilde{u}\tilde{\psi}\,(\tilde{\alpha}_1 - \tilde{\alpha}_2)\,. \tag{3.53}$$

Further rearrangement gives

$$\tilde{u^2}\Delta h' - 2\tilde{u}\Delta\left(h'u^2\right) = \tilde{\psi^2}\Delta h' - \Delta\left(\frac{h'g}{2\cos\theta}\right). \tag{3.54}$$

One way of satisfying equation (3.54) is to make it identically zero on both sides. Thus setting by the right hand side to zero, $\tilde{\psi^2}$ is given by

$$\tilde{\psi^2} = \frac{g}{2\cos\theta}\,(h'_R + h'_L)\,. \tag{3.55}$$

Similarly, solving the quadratic for $\tilde{u}$ gives

$$\tilde{u} = \frac{\Delta\left(h'u\right) \pm \sqrt{\Delta(h'u)^2 - \left(\Delta h'\right)\Delta(h'u^2)}}{\Delta h'} \tag{3.56}$$

and taking the negative value for the second term (the positive value leads to nothing physical), $\tilde{u}$ becomes

$$\tilde{u} = \frac{\sqrt{h'_R}u_R + \sqrt{h'_L}u_L}{\sqrt{h'_R} + \sqrt{h'_L}}. \tag{3.57}$$

From equation (3.56)

$$\Delta(h'u) - \tilde{u}\Delta h' = \sqrt{h'_R h'_L}\Delta u, \tag{3.58}$$

so if $\tilde{h}'$ is defined as $\sqrt{h'_R h'_L}$ then

$$\Delta(h'u) - \tilde{u}\Delta h' = \tilde{h}'\Delta u. \tag{3.59}$$

Having found $\tilde{u}$, $\tilde{\psi}$ for a given $\tilde{h}'$ we now find $\tilde{v}$. Rearranging equation (3.52) yields

$$\Delta(h'uv) = \tilde{v}\tilde{u}\left(\tilde{\alpha}_1 + \tilde{\alpha}_2\right) + \tilde{v}\tilde{\psi}\left(\tilde{\alpha}_1 - \tilde{\alpha}_2\right) + \tilde{u}\tilde{\alpha}_3. \tag{3.60}$$

The wavestrengths can be eliminated by using equations (3.37) to (3.39) with u, v replaced by the interface values and $\sqrt{h^* g}$ replaced by $\tilde{\psi}$. After some rearrangement this gives

$$\Delta(h'uv) - \tilde{u}\Delta\left(h'v\right) = \tilde{v}\left[\Delta(h'u) - \tilde{u}\Delta h'\right]. \tag{3.61}$$

As with equation (3.54) we consider each side of equation (3.61) in turn and set both sides to be zero. Then substituting for $\tilde{u}$ and taking the differences between the states gives

$$\Delta(h'uv) - \tilde{u}\Delta h'v = \tilde{h}'\Delta u\frac{\left(\sqrt{h'_R}v_R + \sqrt{h'_L}v_L\right)}{\sqrt{h'_R} + \sqrt{h'_L}} \tag{3.62}$$

and

$$\tilde{v}\left[\Delta(h'u) - \tilde{u}\Delta h'\right] = \tilde{v}\tilde{h}'\Delta u. \tag{3.63}$$

Combining these two expressions, $\tilde{v}$ is found to be

$$\tilde{v} = \frac{\left(\sqrt{h'_R}v_R + \sqrt{h'_L}v_L\right)}{\sqrt{h'_R} + \sqrt{h'_L}}. \tag{3.64}$$

The approximate values for the wavestrengths are then

$$\tilde{\alpha}_1 = \frac{1}{2}\Delta h' + \frac{\tilde{h}'}{2\tilde{\psi}}\Delta u \tag{3.65}$$

$$\tilde{\alpha}_2 = \frac{1}{2}\Delta h' - \frac{\tilde{h}'}{2\tilde{\psi}}\Delta u \tag{3.66}$$

$$\tilde{\alpha}_3 = \tilde{h}'\Delta v. \tag{3.67}$$

All that remains is to find the values of $\tilde{\beta}_1$, $\tilde{\beta}_2$ and $\tilde{\beta}_3$ that represent the source terms. From

$$\tilde{\mathbf{f}}\left(\mathbf{w}^n\right) = -\frac{1}{\Delta\phi}\sum_{k=1}^{3}\tilde{\beta}_k\tilde{\mathbf{e}}_k \tag{3.68}$$

and from the definition of $\tilde{\mathbf{f}}$

$$\tilde{\mathbf{f}} = \left(0, -\frac{g\tilde{h}'}{a\cos\theta}\frac{\Delta h_s}{\Delta\phi}, 0\right) \tag{3.69}$$

the following are obtained

$$0 = -\frac{1}{\Delta\phi}\left(\tilde{\beta}_1 + \tilde{\beta}_2\right) \tag{3.70}$$

$$-\frac{gh'}{a\cos\theta}\frac{\Delta h_s}{\Delta\phi} = -\frac{1}{\Delta\phi}\left(\tilde{u} + \tilde{\psi}\right)\tilde{\beta}_1 - \frac{1}{\Delta\phi}\left(\tilde{u} - \tilde{\psi}\right)\tilde{\beta}_2 \tag{3.71}$$

$$0 = -\frac{1}{\Delta\phi}\left(\tilde{v}\tilde{\beta}_1 + \tilde{v}\tilde{\beta}_2 + \tilde{\beta}_3\right), \tag{3.72}$$

from which, the corresponding values of $\tilde{\beta}_1$, $\tilde{\beta}_2$ and $\tilde{\beta}_3$ are found to be

$$\tilde{\beta}_1 = \frac{g\tilde{h}'}{a\tilde{\psi}\cos\theta} \tag{3.73}$$

$$\tilde{\beta}_2 = -\frac{g\tilde{h}'}{a\tilde{\psi}\cos\theta} \tag{3.74}$$

$$\tilde{\beta}_3 = 0. \tag{3.75}$$

3.3.2 Applying to the latitudinal (θ) direction

In a manner similar to that applied previously, by writing $\mathbf{G}$ as

$$\mathbf{G} = \left(\frac{n}{a}, \frac{mn}{ah'}, \frac{n^2}{ah'} + \frac{h'^2 g}{2a\cos\theta} \right)^T \tag{3.76}$$

its Jacobian, B, is found to be

$$B = \frac{\partial \mathbf{G}}{\partial \mathbf{w}} = \begin{pmatrix} 0 & 0 & \frac{1}{a} \\ -\frac{uv}{a} & \frac{v}{a} & \frac{u}{a} \\ -\frac{v^2}{a} + \frac{h'g}{a\cos\theta} & 0 & \frac{2v}{a} \end{pmatrix} \tag{3.77}$$

with eigenvalues

$$\lambda_1 = \frac{v}{a} + \frac{\sqrt{h^* g}}{a} \ , \ \lambda_2 = \frac{v}{a} - \frac{\sqrt{h^* g}}{a} \ , \ \lambda_3 = \frac{v}{a} \tag{3.78}$$

and eigenvectors

$$\mathbf{e}_1 = \begin{pmatrix} 1 \\ u \\ v + \sqrt{h^* g} \end{pmatrix} \ , \ \mathbf{e}_2 = \begin{pmatrix} 1 \\ u \\ v - \sqrt{h^* g} \end{pmatrix} \ , \ \mathbf{e}_1 = \begin{pmatrix} 0 \\ 1 \\ 0 \end{pmatrix} \tag{3.79}$$

As before we can find expressions for the interface values of u, v, $\sqrt{h^* g}$ and h' which lead to definitions of $\tilde{\alpha}_1$, $\tilde{\alpha}_2$ and $\tilde{\alpha}_3$ that satisfy

$$\Delta \mathbf{w} = \sum_{k=1}^{3} \tilde{\alpha}_k \tilde{\mathbf{e}}_k \tag{3.80}$$

and

$$\Delta \mathbf{G} = \sum_{k=1}^{3} \tilde{\lambda}_k \tilde{\alpha}_k \tilde{\mathbf{e}}_k. \tag{3.81}$$

Following the algebra through the resulting expression for $\tilde{\psi}^2$ is

$$\tilde{\psi}^2 = \frac{g}{2} \frac{\Delta\left(\frac{h'^2}{\cos\theta}\right)}{\Delta h'} \tag{3.82}$$

However unlike last time, $\cos\theta$ will be different for the two states. Because $\tilde{\psi}$ must be a real quantity, as it approximates $\sqrt{h^* g}$, it is necessary that $\tilde{\psi}^2$ be positive. This can be ensured by replacing the left and right values of $\cos\theta$ with an average value, for example the value of $\cos\theta$ at the interface. Thus $\tilde{\psi}^2$ becomes

$$\tilde{\psi}^2 = \frac{g}{2\cos\theta_I}\left(h'_R + h'_L\right) \tag{3.83}$$

where $\theta_I = \frac{1}{2}\left(\theta_L + \theta_R\right)$. We find that $\tilde{u}$ and $\tilde{v}$ are the some as in the previous case, namely

$$\tilde{u} = \frac{\sqrt{h'_R}u_R + \sqrt{h'_L}u_L}{\sqrt{h'_R} + \sqrt{h'_L}} \tag{3.84}$$

and

$$\tilde{v} = \frac{\left(\sqrt{h'_R}v_R + \sqrt{h'_L}v_L\right)}{\sqrt{h'_R} + \sqrt{h'_L}}. \tag{3.85}$$

Setting $\tilde{h}' = \sqrt{h'_L h'_R}$ results in the following expressions for the wavestrengths

$$\tilde{\alpha}_1 = \frac{1}{2}\Delta h' + \frac{\tilde{h}'}{2\tilde{\psi}}\Delta v \tag{3.86}$$

$$\tilde{\alpha}_2 = \frac{1}{2}\Delta h' - \frac{\tilde{h}'}{2\tilde{\psi}}\Delta v \tag{3.87}$$

$$\tilde{\alpha}_3 = \tilde{h}'\Delta u. \tag{3.88}$$

As before the source term is projected onto the local eigenvectors. Defining $\tilde{\mathbf{g}}$ as

$$\tilde{\mathbf{g}} = \left(0, 0, -\frac{g\tilde{h}'}{a}\frac{\Delta h_s}{\Delta\theta}\right)^T \tag{3.89}$$

and using

$$\tilde{\mathbf{g}}\left(\mathbf{w}^n\right) = -\frac{1}{\Delta\phi}\sum_{k=1}^{3}\tilde{\beta}_k\tilde{\mathbf{e}}_k \tag{3.90}$$

leads to the values of $\tilde{\beta}_1$, $\tilde{\beta}_2$ and $\tilde{\beta}_3$ being

$$\tilde{\beta}_1 = \frac{g\tilde{h}'}{a\tilde{\psi}\cos\theta} \tag{3.91}$$

$$\tilde{\beta}_2 = -\frac{g\tilde{h}'}{a\tilde{\psi}\cos\theta} \tag{3.92}$$

$$\tilde{\beta}_3 = 0. \tag{3.93}$$

Chapter 4

The test case and computational considerations

4.1 The test case

The test case to which we shall apply the method is the first problem in a suite of seven cases proposed by Williamson et al [13], developed specifically for the shallow water equations.

The problem entails predicting the motion of a cosine bell over the globe, and tests the advective part of any scheme, by specifying analytic values for the advecting winds. Different wind directions are used, which alter the path of the bell.

The advecting wind is given by

$$u = u_0 \left(\cos\theta \cos\alpha + \sin\theta \sin\alpha\right) \tag{4.1}$$

$$v = -u_0 \sin\phi \sin\alpha, \tag{4.2}$$

where α is the angle between the axis of solid body rotation and the polar axis

of the spherical coordinate system.

In the paper it suggests running the code with $\alpha = 0.0,\ 0.05,\ \pi/2 - 0.05$ and $\pi/2$. With α set to zero, the profile moves around the equator. For α equal to $\pi/2$, the trajectory is over the poles.

The initial cosine bell is defined by

$$h^*(\phi,\theta) = \begin{cases} \frac{h_0^*}{2}\left(1+\cos\left(\frac{\pi r}{R}\right)\right) & \text{if } r < R \\ 0 & \text{if } r \geq R \end{cases}, \tag{4.3}$$

where $h_0^* = 1000m$, $R = a/3$ and r is the radius of the great circle distance between (ϕ,θ) and the centre of the bell which is initially at $(\phi_c,\theta_c) = (3\pi/2, 0)$. The radius r can be calculated from

$$r = a\cos^{-1}\left[\sin\theta_c\sin\theta + \cos\theta_c\cos\theta\cos\left(\phi-\phi_c\right)\right]. \tag{4.4}$$

The parameter values to be used are

$$a = 6.37122\times 10^6 m$$

$$\Omega = 7.292\times 10^5 s^{-1}$$

$$g = 9.80616 m s^{-2}$$

and u_0 is to be set as $2\pi a/(12 \text{ days})$ which is equivalent to about $40 m s^{-1}$. There are no mountains in this problem, corresponding to h_s being zero everywhere.

If the program is run for 12 days then the initial profile should have returned to its starting point, without any change of shape.

4.2 The grid

The grid we shall use has points equally distributed in the longitudinal and latitudinal directions, with grid spacings $\Delta\phi$ and $\Delta\theta$ respectively. In this instance

the angle θ is not the standard polar coordinate but is instead measured from the equator so that θ lies in the interval $[-\pi/2, \pi/2]$ where $-\pi/2$ is the South pole and $\pi/2$ is the North pole.

There are no nodes at the poles, nodes which lie directly opposite one another closest the poles being $\frac{1}{2}\Delta\theta$ from the pole. To avoid nodes at the pole points, it becomes necessary that there are an even number of intervals in the longitudinal direction.

4.3 Stability analysis

For an equation of the form

$$w_t + a u_x = 0 \tag{4.5}$$

the stability (CFL) condition is

$$\left| a \frac{\Delta t}{\Delta x} \right| \leq 1. \tag{4.6}$$

In this instance, there are two stability conditions [4] which must both be satisfied. These are

$$\left| \frac{\tilde{\lambda}_{max}}{a \cos\theta} \frac{\Delta t}{\Delta \phi} \right| \leq 1 \tag{4.7}$$

for the ϕ direction, and

$$\left| \frac{\tilde{\lambda}_{max}}{a} \frac{\Delta t}{\Delta \theta} \right| \leq 1 \tag{4.8}$$

for the θ direction, where $\tilde{\lambda}_{max} = \max(\tilde{\lambda}_1, \tilde{\lambda}_2, \tilde{\lambda}_3)$ for the two problems.

From the definitions of the approximate eigenvalues for the two directions, we see that condition (4.7) imposes a more severe constraint on the time step than condition (4.8) especially as the profile tends towards the poles where $\cos\theta \to 0$.

Chapter 5

Results

5.1 Translation of the bell around the equator

The first figure shows a contour plot of the initial height of the cosine bell, where $h = h^*$ with the centre positioned at $(\phi, \theta) = (\frac{3\pi}{2}, 0)$ with a peak value of 1000m.

Running the program for 12 days with $\alpha = 0$ on a 96×73 grid using a time step of $1800s$ produces figure 2. Although the centre of the bell has returned to its initial position and the contour plots show the profile to be almost symmetric, a large amount of diffusion has taken place (as expected), as can be seen by the fact that the profile has spread out and that the peak value has decreased dramatically. It is expected that refining the grid would reduce this problem and as figure 3 shows where the grid spacing has been halved, this turns out to be the case.

To investigate how much the size of the time step contributes to the diffusion, the program is run with $\Delta t = 450s$, as shown in figure 4. From comparison with figure 2, we deduce that the size of the time step is not a contributing factor to

the diffusion problem as figures 2 and 4 are almost identical.

The results so far suggest that it would be wise to introduce a flux limiter into the code [12]. Using Roe's 'superbee' limiter [9], the amount of diffusion is greatly reduced, as demonstrated by comparing figure 5 with figure 2, where the two runs are performed on the same grid. In figure 2 we see that the peak height has been reduced to about 65, whereas in figure 5 the reduction is much less, and the peak value is about 500. However an offset to this improvement is the need for a smaller time step, as it is found that using $\Delta t = 1800s$ gives an unstable solution. We also observe that the use of operator splitting has resulted in the 'squaring' of the solution. This can be seen by the way in which the contour lines have become almost parallel with the grid lines. This is more evident in the results using the limiter as the profile is less diffused here. However it can also be seen that in the latitudinal direction the profile has maintained its original width. Another noticeable effect is the extra steepening of the profile on the right hand side.

Repeating the run with the same values but this time using Roe's 'minmod' [9] limiter gives figure 6. Although the results are better than when no limiter was used, in this case it is evident that the superbee limiter is superior than the minmod limiter in reducing the amount of diffusion.

Figures 7 and 8 show the results when both limiters are implemented on a 192×146 grid using a time step of 450s. As seen before using a finer grid reduces the amount of diffusion, and the steepening effect is less evident when the mesh spacings are reduced as a result.

A further improvement is seen in figures 9 and 10 where Strang splitting is

used to decompose the system of equations. Though the squaring effect is still present, the maximum height values are much better than before.

When the program is run using $\alpha = 0.05$, the results produced are very similar to those already seen and so are not included here.

For all the runs we see that the profile has been elongated along the direction of the flow. There are no oscillations or negative heights present, and the solution remains smooth.

There are a multitude of papers on the solutions of the shallow water equations on a sphere which consider a variety of methods and give many results. We shall only draw a comparison with a few other methods here which have also been applied to the first test case in [13].

In [7] Malcolm applies a number of schemes to the shallow water equations using the first test case of Williamson et al. The results presented were obtained using a similar latitude/longitude grid to that used here. Note that in the plots the values of the height have been scaled up by 1000. The results in figure 11 were obtained using the unified model advection scheme. The contour lines lie in the range 700-1700, corresponding to the presence of negative values for the height using the normal scale. This is a result of the oscillations present. Better solutions were obtained using the $4th$ order Heun scheme. Figure 12 shows the solution on a 96×73 grid. The peak value has only decreased slightly, again negative values have appeared due to the oscillations occurring along the path that the bell took, and the profile steepened on the left hand side. Using a 288×217 grid the results were improved corresponding to the maximum and minimum height values being raised, and the profile being symmetric about the

line $\phi = 3\pi/2$. Further results were obtained from Heun's scheme incorporating the use of a filtering technique and using both $4th$ and $6th$ order diffusion terms. Shown also are the results from using a semi-lagrangian code. We quote in table 1 below the maximum and minimum values attained for the height profiles for some different schemes on a 96×73 grid with a 30 minute time step. Included within the table are some results obtained using a similar TVD scheme to that used here.

Scheme	Max. height	Min. height
Heun scheme	1937.5	836.4
Heun scheme + 4th order diffusion	1707.3	955.1
TVD (superbee)	1739.5	1000.0
TVD (van leer)	1540.0	1000.0

Table 1:

In a publication by Heikes [5] a new model was presented for the shallow water equations which solves the stream function/velocity potential form of the equations on a new grid. In the paper the results from this model were compared to those obtained using the Arakawa-Lamb and NCAR spectral shallow water models (which both use regular longitudinal/latitudinal grids) on the Williamson et al test cases. Figures 14 and 15 are the results from running the proposed model and the Arakawa-Lamb model on the first test case. In both models elongation of the profiles occurred in the direction of the flow. In this instance the solution obtained using the NCAR model is identical to the initial conditions [6].

5.2 Translation of the bell over the poles

The next part of the test is to send the profile over the poles. Because of the need for a much smaller time step than before (in order to satisfy the stability condition), the overall running time is increased, and so only 6 day runs will be performed. With the values of u and v given with $\alpha = \pi/2$ this should carry the bell over the North Pole and place the centre at $(\pi/2, 0)$.

Running the code on a 60×30 grid without any limiters gives figure 16. Here the time step is 5s. From the stability condition, this value for Δt should have given an unstable solution. However as a large amount of diffusion had already taken place by the time the profile reached the pole, the values of $\tilde{\lambda}_{max}$ at this time were less than the initial values, and so as, a result of the diffusion, we can get away with using a larger time step than the stability condition would predicted. The results using a 96×73 are shown in figure 17,and as expected there is an improvement on the solution shown in figure 16. Using the superbee limiter we see again the squaring effect, and reduction of the diffusion. It is apparent that the centre of the cone has not been conveyed to the equator. In the results produced by Heikes [5] the profile is very similar in shape to the results he obtained using $\alpha = 0$

Chapter 6

Conclusion

Roe's method for the solution of a set of conservation laws was considered in chapter 2. In chapter 3 we took the standard flux form of the shallow water equations on a sphere, and through a series of manipulations transformed the equations into a set of conservation laws. We then went on to apply the technique known as operator splitting to decompose the system of conservation laws into two one dimensional problems. We then proceeded to solve these equations numerically using Roe's scheme. A test case was then presented in chapter 4, the solutions to which were shown in chapter 5.

From the results produced within this dissertation a number of important conclusions can be drawn. We saw that when Roe's scheme was used in isolation the solutions were very diffused. However the introduction of a flux limiter reduced the effects of the diffusion dramatically. Of the limiters tried, Roe's superbee limiter gave the best results. The use of limiters introduced some new problems, namely the exaggeration of squaring of the solutions and the need for a smaller time step than when no limiters were used. In all cases the profile was seen to

be stretched in the direction of the flow corresponding to different parts of the solution travelling with different phase speeds. We found that a very small time step had to be used to send the bell over the pole, because of the large wavespeeds in the ϕ direction, so that the solution remained stable. The form of splitting used to decompose the equation affected the quality of the solution, in particular we saw that using Strang splitting gave better results than when the simpler form of operator splitting was used.

From a comparison with some other methods we have seen that the problem of the solution being stretched along the flow direction is a common problem to many methods. Although Roe's scheme is only first order and so very diffusive, we were able to reduce this problem by using flux limiters, but not to the extent that we could produce comparable results to some of the more accepted methods. We saw that one of the major problems encounted with some other methods, the presence of oscillations in the solution, was not a problem in this instance.

From the difficulties encountered with the small step size near the pole there is an obvious need to use an implicit scheme to which the size of the time step is not restricted by a stability condition, if a regular latitude/longitude grid is to be used. Alternatively, perhaps the pole problem could be overcome by using a non-regular grid where the grid points do not bunch together at the poles. It might be possible to write an adaptive code which modifies the size of the time step depending on the solution, so that at all times the maximum time step is used that will satisfy the CFL condition. However, although that would produce

a faster code when applied to this particular test case, it would not in practice be more efficient for a general problem. So far only the advective part of the code has been tested. To give a true evaluation of the methods performance further testing is needed.

Acknowledgements

I would like to thank Dr. M. J. Baines, Dr. P. K. Sweby and Dr. P. Glaister of the Mathematics Department, University of Reading, and Dr. N. Nikiforakis of the University of Cambridge and UGAMP, for their help, support and advice during this work. Thanks also to Dr. A. J. Malcolm and Mr. M. E. Hubbard for their assistance. I would also like to acknowledge the financial support of EPSRC.

Bibliography

[1] Courant R., Isaacson E., Rees M., 1952: On the solution of non-linear hyperbolic differential equations by finite differences. Communications in Pure and Applied Mathematics, **5**, 243-249.

[2] Glaister P. 1985: Flux difference splitting techniques for the Euler equations in non-cartesian geometry. Numerical Analysis Report 8-85, University of Reading.

[3] Glaister P., 1987: Difference schemes for the shallow water equations. Numerical Analysis Report 9-87, University of Reading.

[4] Haltimer G. J., Williams R. J., 1980: Numerical prediction and dynamic meteorology, 2nd ed. (Wiley, New York)

[5] Heikes R., 1993: The shallow water equations on a spherical geodesic grid. Colorado State University, Department of Atmospheric Science, **524**.

[6] Jakob R., Hack J. J., Williamson D. L., 1993: Solutions to the shallow water test set using the spectral transform method. NCAR Technical Note NCAR/TN-388+STR

[7] Malcolm A. J., 1994: Testing advection schemes for the shallow water equations on a set of test problems. Forcasting Research Division Technical Note No. **83**, Meteorological Office, Bracknell.

[8] Roe P. L., 1981: Approximate Riemann solvers, parameter vectors, and difference schemes. Journal of Computational Physics, **43**, 357-372.

[9] Roe P. L., Baines M. J., 1982: Alogorithms for advecting shock problems. Proceedings of the Fourth GAMM Conference on Numerical Methods in Fluid Mechanics, Ed. H. Viviand (Vieweg), **5**, 281-290.

[10] Roe P. L., Baines M. J., 1983: Asymptotic behaviour of some non-linear schemes for linear advection. Proceedings of the Fifth GAMM Conference on Numerical Methods in Fluid Mechanics, Ed. M. Pandolfi and R. Piva, (Vieweg), **7**, 283-290.

[11] Roe P. L., 1986: Characteristic-based schemes for the Euler equations. Annual Review of Fluid Mechanics, **18**, 337-365.

[12] Sweby P. K. 1984: High resolution schemes using flux limiters for hyperbolic conservation laws. SIAM Journal of Numerical Analysis, **21**, 995-1011.

[13] Williamson D. L., Drake J. B., Hack J. J., Jakob R., Swarztrauber P. N., 1992: A standard test set for numerical approximations to the shallow water equations in spherical geometry. Journal of Computational Physics, **102**, 211-223.

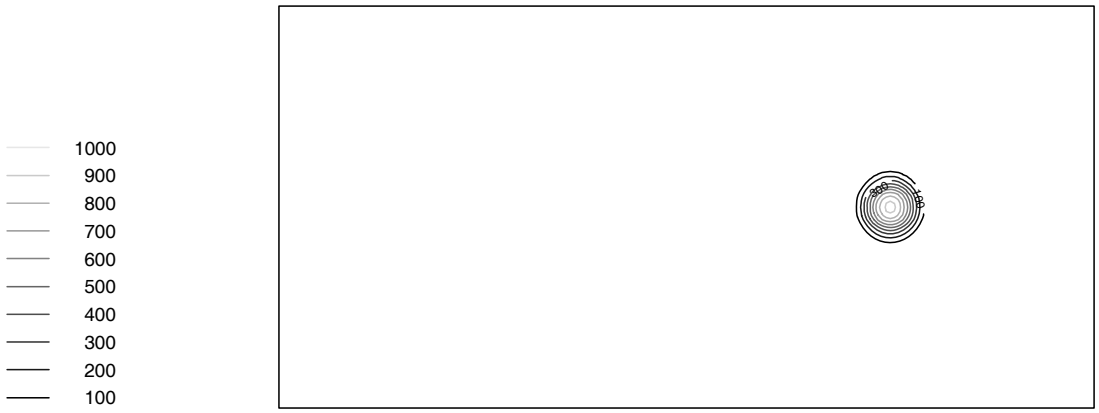

Figure 1: Initial data

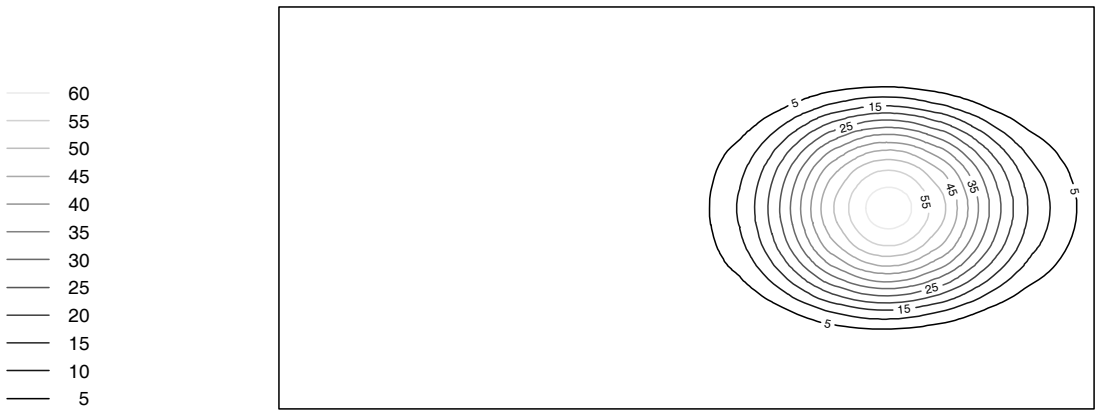

Figure 2: $\alpha = 0$, 96×73, $\Delta t = 1800s$

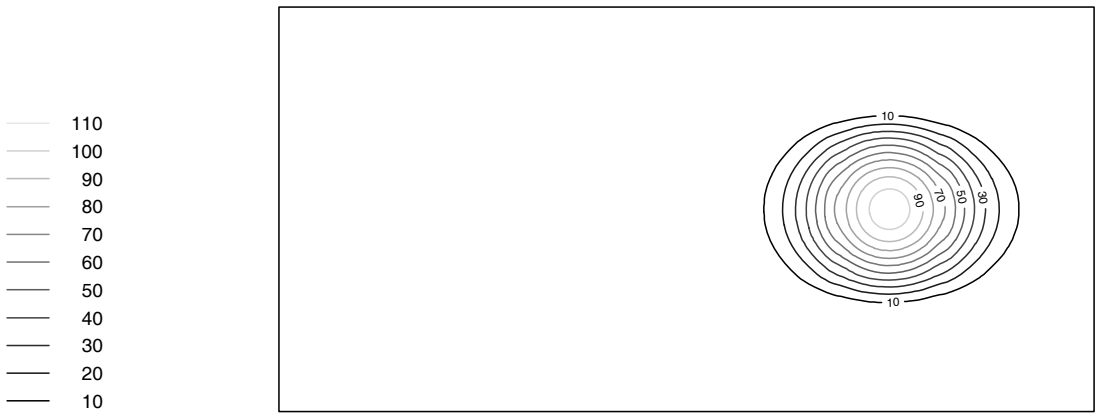

Figure 3: $\alpha = 0$, 192×143, $\Delta t = 900s$

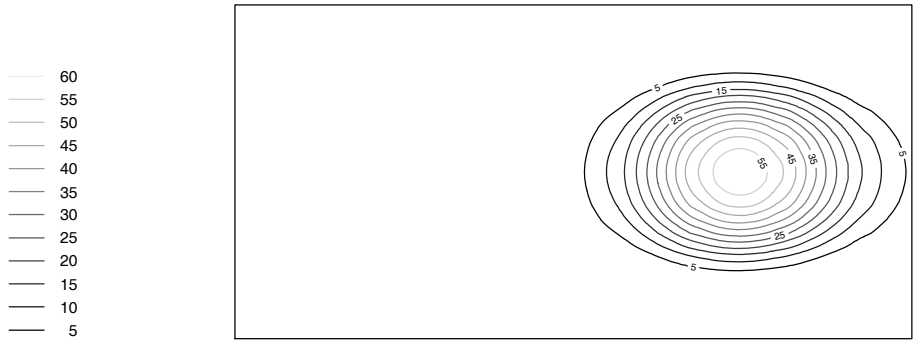

Figure 4: $\alpha = 0$, 96×73, $\Delta t = 450s$

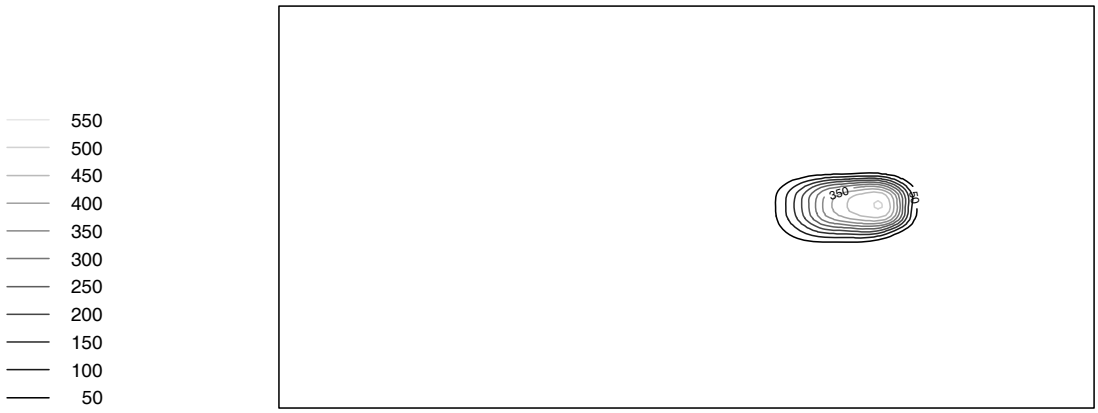

Figure 5: $\alpha = 0$, 96×73, $\Delta t = 900s$, Superbee

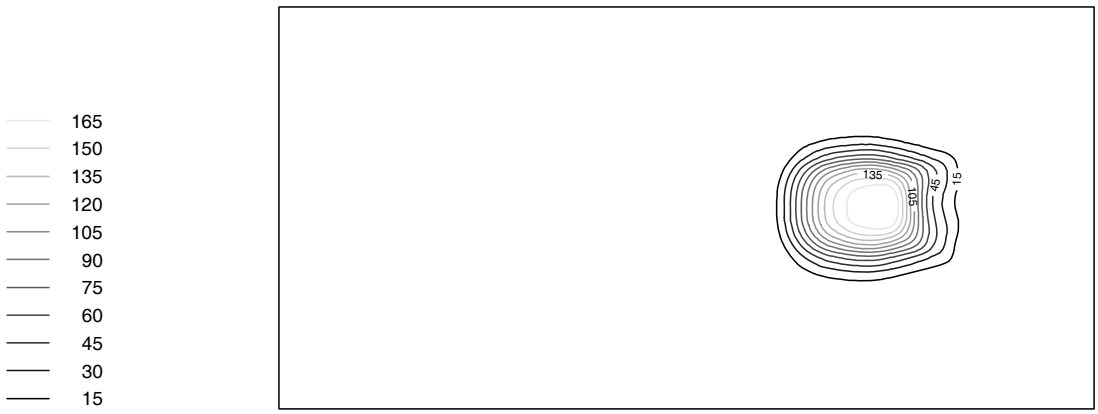

Figure 6: $\alpha = 0$, 96×73, $\Delta t = 900s$, Minmod

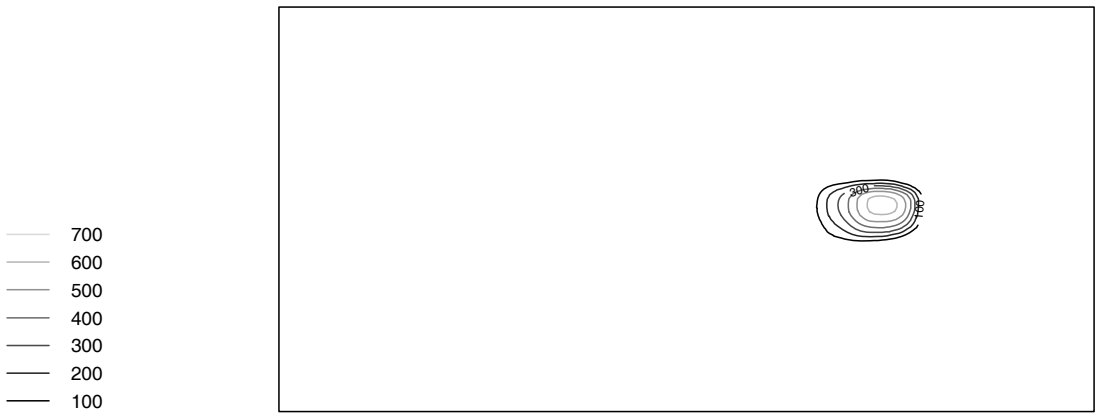

Figure 7: $\alpha = 0$, 192×146, $\Delta t = 450s$, Superbee

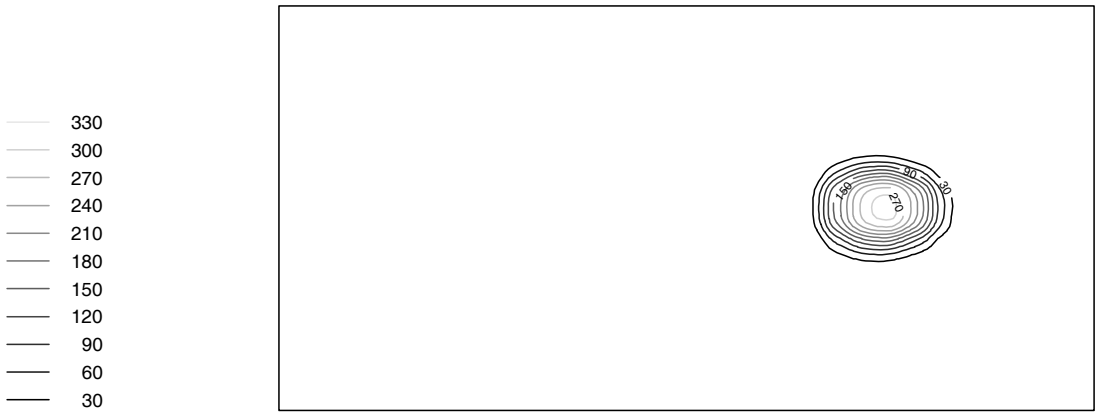

Figure 8: $\alpha = 0$, 192×146, $\Delta t = 450s$, Minmod

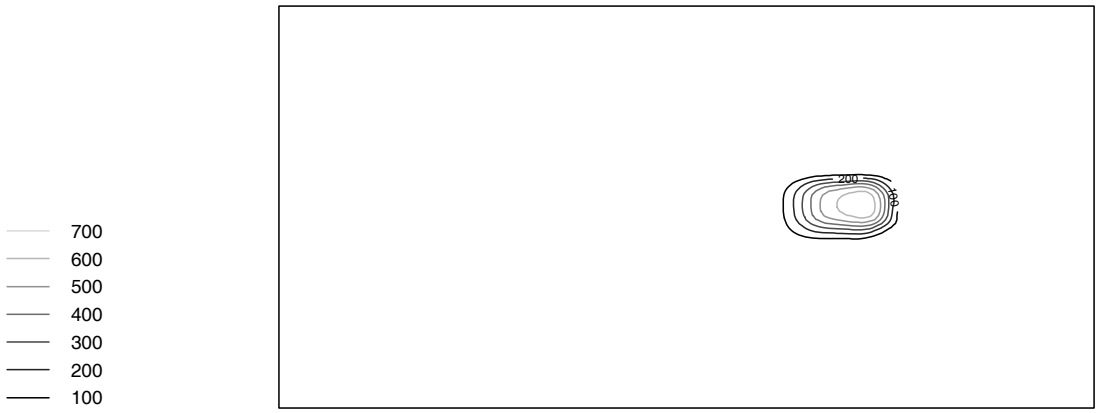

Figure 9: $\alpha = 0$, 96×73, $\Delta t = 900s$, Strang splitting with Superbee

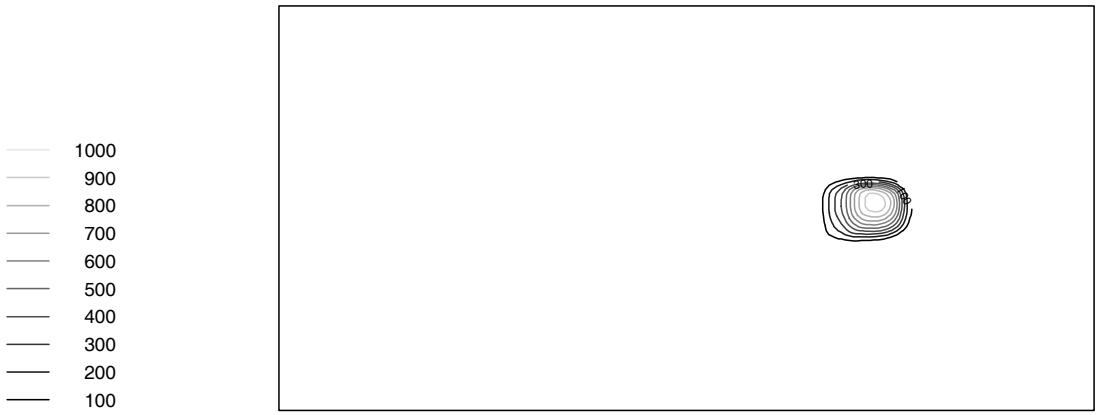

Figure 10: $\alpha = 0$, 192×146, $\Delta t = 450s$, Strang splitting with Superbee

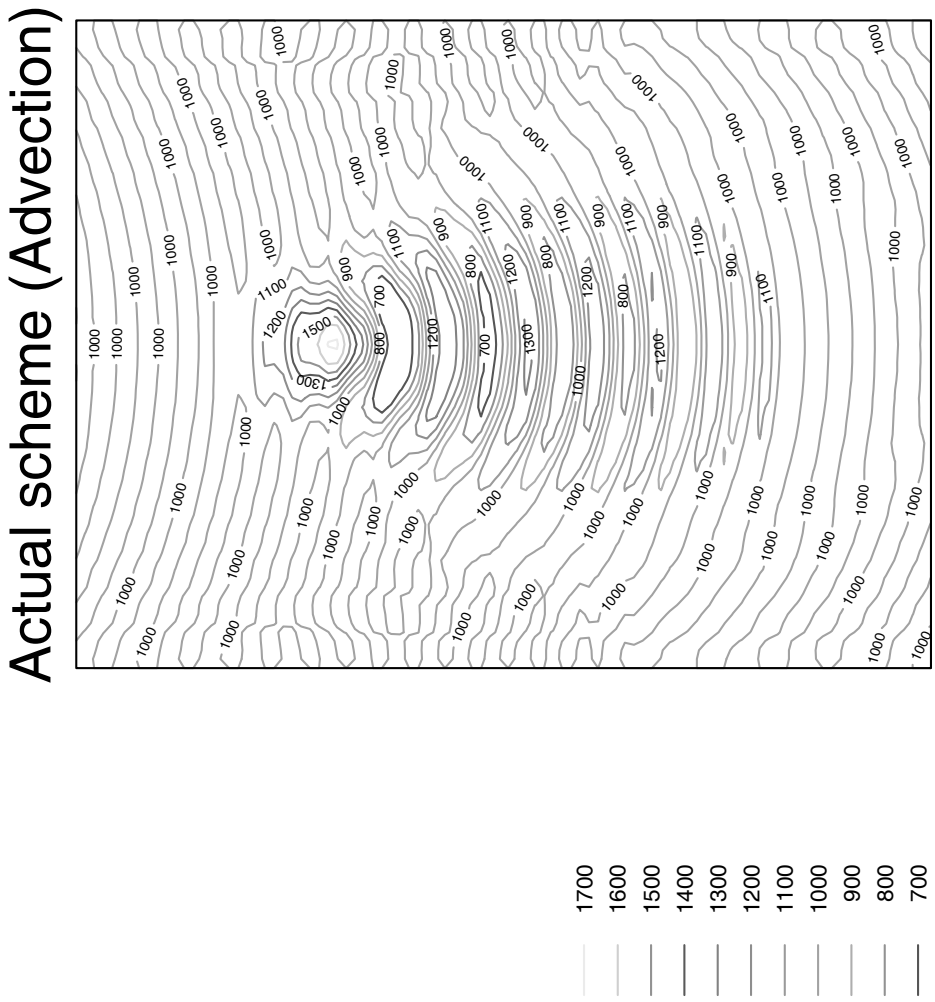

Figure 11: Unified model: $\alpha = 0$, 96×73, $\Delta t = 1800s$

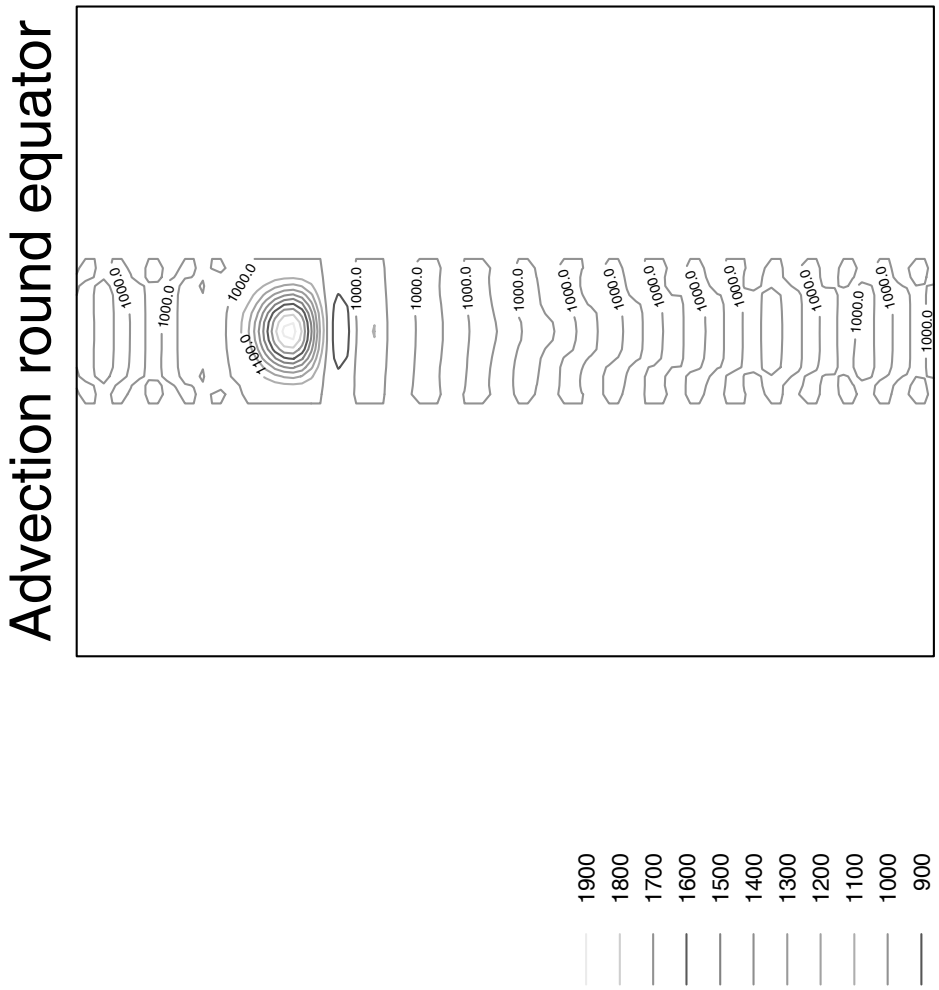

Figure 12: Heun scheme: $\alpha = 0$, 96×73, $\Delta t = 1800s$

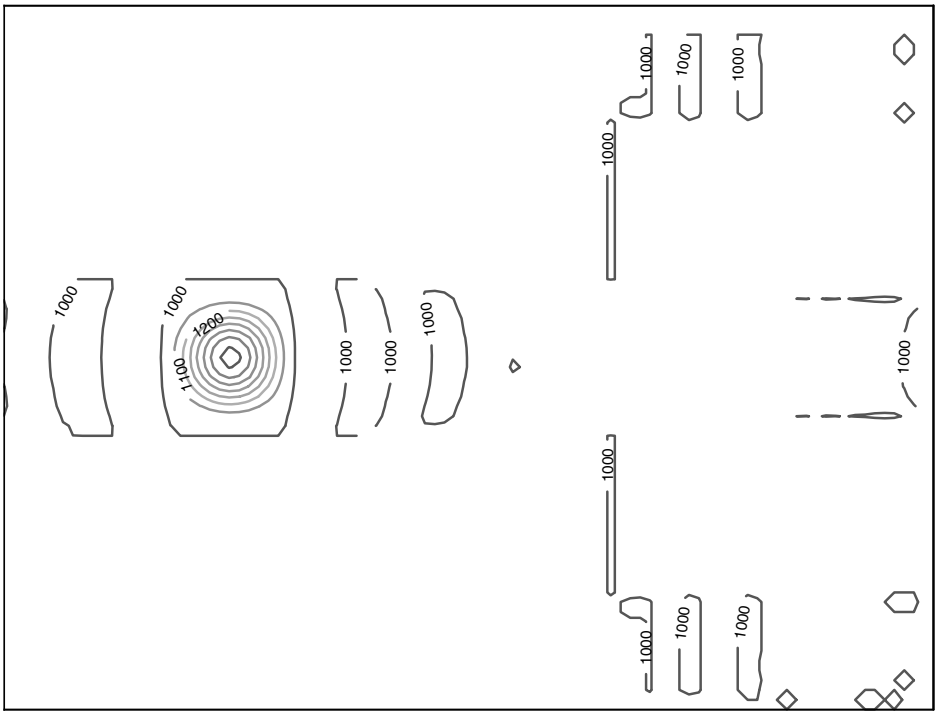

Figure 13: Semi-lagrangian: $\alpha = 0$, 96×73, $\Delta t = 1800s$

Figure 14: TIG-2562: $\alpha = 0$, a.) Day 3, b.) Day 6, c.) Day 9, d.) Day 12.

Figure 15: Arakawa-Lamb: $\alpha = 0$, a.) Day 3, b.) Day 6, c.) Day 9, d.) Day 12.

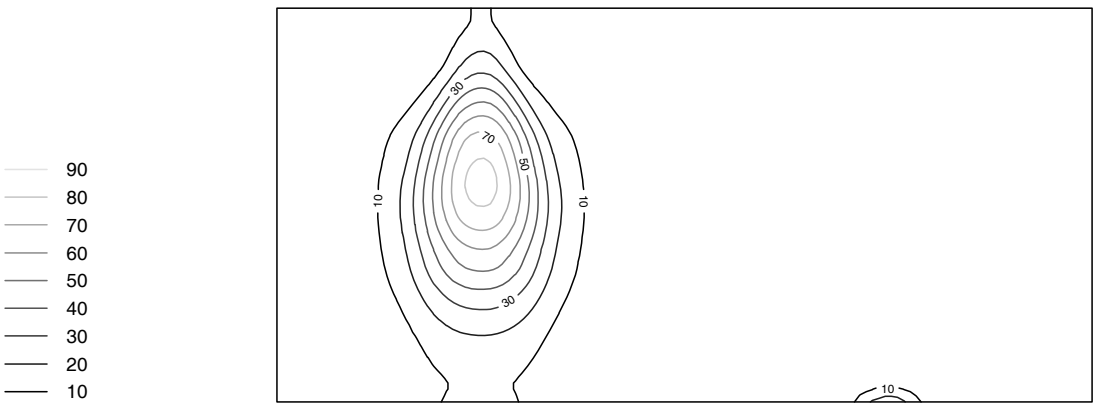

Figure 16: $\alpha = \frac{\pi}{2}$, 60×30, $\Delta t = 5s$

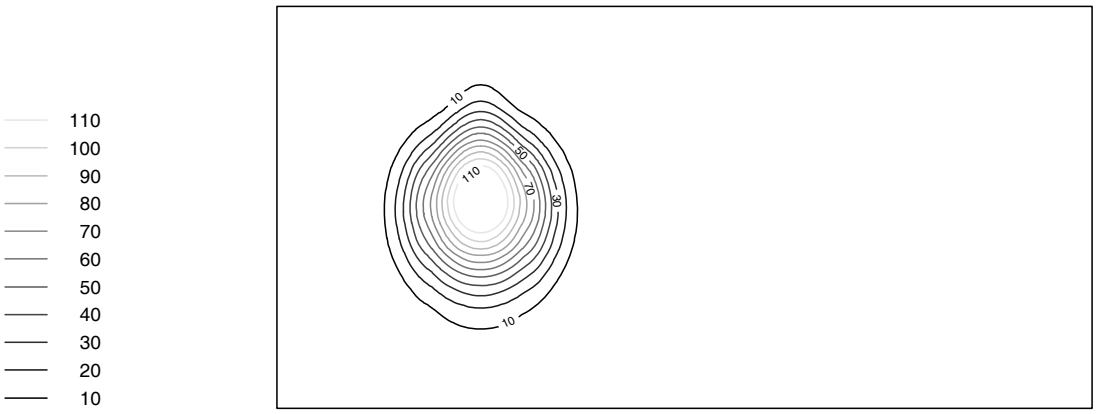

Figure 17: $\alpha = \frac{\pi}{2}$, 96×73, $\Delta t = 1s$

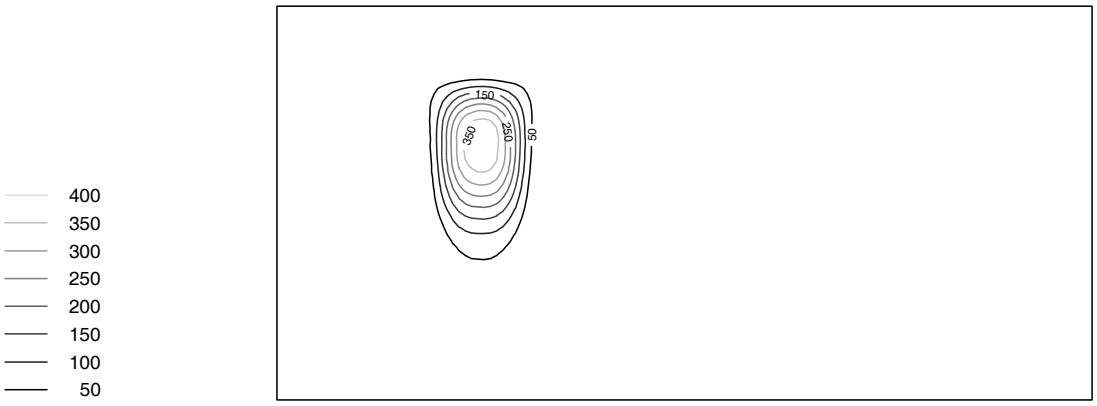

Figure 18: $\alpha = \frac{\pi}{2}$, 60×30, $\Delta t = 1s$, Superbee